

Pulsed quantum annealing

Vasilios Karanikolas* and Shiro Kawabata†

Device Technology Research Institute, National Institute of Advanced Industrial Science and Technology (AIST),
Tsukuba, Ibaraki 305-8568, Japan

We propose a modified quantum annealing protocol, *i.e.*, *pulsed quantum annealing* (PQA), in order to increase the success probability by a pulse application during the quantum annealing process. It is well known that the success probability of the conventional quantum annealing is reduced due to the Landau-Zener transitions. By applying a pulse to the system, we modulate the success probability and increase it, compared to the conventional quantum annealing, by optimizing the pulse parameters. We demonstrate our findings for a single qubit both numerically and analytically. The analytical model is based on the transfer matrix approach and it is in good agreement with the full numerical results. We also investigate the PQA protocol for multi-qubit cases *i.e.*, random spin-glass instances, and we present an overall increase of the success probability over the conventional quantum annealing, by optimizing the pulse parameters. Our results indicate that PQA can be used to design future high-performance quantum annealing machines, especially for hard instances that the conventional QA protocol behaves poorly.

1. Introduction

Quantum annealing (QA) has been introduced as an alternative to simulated annealing for efficiently solving combinatorial optimization problems.^{1,2)} The advantage of QA over the classical simulated annealing³⁾ is that during the annealing, the search for the optimum state of the system can stuck to a local minima, then quantum fluctuations can help the system to tunnel from the local minima to the global one.⁴⁾ The research on QA is intensified in recent years, after the commercialization of the QA machines by D-Wave Systems Inc. using superconducting flux qubits.^{5–7)} The QA machines from D-Wave Inc. have been used in a number of diverse hard optimization problems, to name a few: global warming,⁸⁾ traffic control,⁹⁾ election forecasting,¹⁰⁾ online advertisement allocation,¹¹⁾ and analyzing data regarding the Higgs boson discovery from Large Hadron Collider.¹²⁾ In addition, new quantum annealing machines are now developed by several groups.^{13–20)}

The adiabatic theorem guaranties that if the annealing process is slow enough the final state will be the ground state of the problem Hamiltonian, thus a solution of an optimization problem. The annealing time is inversely proportional to energy gap between the ground and the first excited state.²¹⁾ Hence, optimization problems with extremely small energy gap demand long annealing times. However, long annealing times reduces the success probability (SP) due to coupling of the qubits with the environment and decoherence.²²⁾ As SP is defined the probability of the instantaneous ground state of the Hamiltonian at the end of the annealing. Thus, SP measures how close we are to the optimum solution. On the same time, for spin glass problems it has been found that decreasing the annealing time can be beneficial.^{23,24)} The physical explanation is that for fixed annealing times the state can stuck in a local minima, and by reducing the annealing time, non-adiabatic processes are introduced that can kick the system

from the local minima of the system, to the global minimum. Thus, an induced nonadiabatic process can be used to increase the SP.

Importantly, the QA is closely connected with the Landau-Zener physics.²⁵⁾ The transition probability at avoided energy level crossings between the ground and first excited state has been investigated intensively.²⁶⁾ Vitanov *et al.*, have showed that a diabatic pulsed quantum fluctuation during the Landau-Zener transition causes an oscillatory behavior of the transition probability.²⁷⁾

In this paper we introduce the *pulsed quantum annealing* (PQA) protocol. By applying a single pulse to the system during the quantum annealing process, we can modulate the SP and increase it in comparison with the conventional quantum annealing, for a set of pulse parameters. Starting from the single qubit case, we analytically show that this modulation can be explained by the destructive and constructive interference model based on the transfer matrix approach.^{28–30)} To our knowledge, that is the first time that this semianalytical model is used to describe the quantum annealing protocol. In addition, we also numerically investigate PQA for multi-qubit cases and confirm the enhancement of SP by optimizing pulse parameters over multiple random instances.

The paper is organized as follow. In Sec.2 we consider the PQA protocol for a single qubit. We present the transfer matrix method,²⁸⁾ using the sudden approximation, and compare it with full numerical results. In Sec.3 we apply PQA for multi-qubit cases. We show that for any instance generated, for certain pulse parameters, the SP is increased, compared to conventional QA. In Sec.4 we give the concluding remarks and discuss possible future directions. In Appendix A we present in more details the transfer matrix method using the sudden approximation.

*Present address: International Center for Young Scientists (ICYS), National Institute for Materials Science (NIMS) 1-1 Namiki, Tsukuba, Ibaraki 305-0044, Japan. E-mail: KARANIKOLAS.Vasileios@nims.go.jp

†Corresponding author. E-mail: s-kawabata@aist.go.jp

2. Pulsed quantum annealing for a single qubit

2.1 Transfer-matrix approach to describe the pulsed quantum annealing for a single qubit

The Hamiltonian describing the PQA protocol for a single qubit, including the applied pulse, has the form,

$$H(t) = \left[\frac{t}{t_f} \varepsilon + C \Lambda_P(t) \right] \sigma_z + \left[1 - \frac{t}{t_f} \right] \Delta \sigma_x, \quad (1)$$

where σ_z and σ_x are the Pauli matrices, t_f is the annealing time, Δ gives the strength of the quantum fluctuations, ε is the energy difference between the $|0\rangle$ and $|1\rangle$ states in the diagonal term and C is the strength of the applied diabatic pulse. $\Lambda(t) = \Theta(t - t_C + t_D/2) \Theta(t_C + t_D/2 - t)$ is the pulse shape, in the diagonal part, which is characterized by the pulse center t_C and the pulse duration t_D ; where the theta function is defined as $\Theta(x) = 1$ if $x > 0$. Through out this paper we use energy units expressed through Δ , thus the time scales are expressed in \hbar/Δ units. When there is no applied pulse we have the conventional linear ramp QA, which is characterized by the usual Landau-Zener physics at the avoided crossing. Throughout this paper we focus on cases where the temperature is well below the minimum energy gap, $E_G^{\min} \gg k_B T$, thus we take the zero temperature limit, $T = 0K$.

Our approach consists of solving numerically the time-dependent Schrödinger equation

$$i\hbar \frac{\partial}{\partial t} |\psi(t)\rangle = H(t) |\psi(t)\rangle, \quad (2)$$

which is used to simulate the QA process, with and without the diabatic pulse. Also, the exact diagonalization of the Hamiltonian $H(t)$ (1), without the applied pulse, is used to calculate its instantaneous eigenstates $|\psi_i(t)\rangle$, for $i = 0, 1, \dots, 2^n - 1$, for n qubit systems. At the end of the annealing, $t = t_f$, we define the SP as the projection of the instantaneous ground state $|\psi_0(t_f)\rangle$ to the system state $|\psi(t_f)\rangle$

$$P = \left| \langle \psi_0(t_f) | \psi(t_f) \rangle \right|^2. \quad (3)$$

The conventional adiabatic QA protocol has to fulfill the adiabatic condition²¹⁾

$$t_f \gg \frac{\max_{0 \leq s \leq 1} \left| \langle \psi_0(s) | \frac{dH(s)}{ds} | \psi_1(s) \rangle \right|}{\min_{0 \leq s \leq 1} [E_{01}(s)]^2}, \quad (4)$$

for completely reducing unwanted Landau-Zener transitions, where $s = t/t_f$, $|\psi_i(s)\rangle$ describe the ground, $i = 0$, and first, $i = 1$, excited instantaneous eigenstates of the Hamiltonian Eq. (1), without the pulse term, and $E_{01}(s)$ the energy difference between them. The physical meaning of Eq. (4) is that the annealing process should be long enough for suppressing undesired Landau-Zener transitions.

The energy difference between the ground and the excited states of Eq. (1) is given by $E_G(t) = 2\sqrt{(1 - t/t_f)^2 \Delta^2 + (t/t_f \varepsilon + C \Lambda_P(t))^2}$ and is plotted in Fig. 1 for the case of $t_f = 10\hbar/\Delta$ and $\varepsilon = 1\Delta$ with the pulse, continuous line, and without the pulse, dashed line. The pulse parameters are $t_C = 5\hbar/\Delta$, $t_D = 5\hbar/\Delta$ and $C = 1\Delta$. We observe that the pulse application has split the time evolution path of the qubit's states in three parts, denoted by the times $t_{1,2} = t_C \pm t_D/2$, defining the pulse application.

The pulse application is a fast diabatic process, which vio-

lates the adiabatic condition at the pulse application times t_1 and t_2 . Away from t_1 and t_2 , in the regions $j = A_1, A_2, A_3$, the qubit follows essentially an adiabatic evolution path as long as Eq. (4) is satisfied. Then, the time dependent state of the single qubit, described by the state vector $\mathbf{b}(t) = \begin{pmatrix} b_0(t) \\ b_1(t) \end{pmatrix}$ (see Appendix A), during these regions can be found by $\mathbf{b}(t_q) = U_j(t_q, t_s) \mathbf{b}(t_s)$, where $j = A_1, A_2, A_3$. The unitary evolution matrix is defined as

$$U_j(t_q, t_s) = \begin{pmatrix} e^{-i\zeta_j(t_q, t_s)} & 0 \\ 0 & e^{i\zeta_j(t_q, t_s)} \end{pmatrix} = e^{-i\zeta_j(t_q, t_s) \sigma_z}, \quad (5)$$

where

$$\zeta_j(t_q, t_s) = \int_{t_s}^{t_q} E_G(t) dt, \quad (6)$$

is the phase acquired during the adiabatic evolution in regions $j = A_1, A_2, A_3$. The acquired phases $\zeta_j(t_q, t_s)$ have a geometrical interpretation, they are connected with the area below the curve in Fig. 1. t_s and t_q define the start and finish times at each region A_1, A_2 and A_3 .

At times t_1 and t_2 the Hamiltonian changes rapidly due to the pulse application; the change is so sudden that the system does not have time to readjust its state,³¹⁾ thus the qubit state at t_l^+ can be written in terms of the state at t_l^- , for $l = 1, 2$, where t_l^+ are the times right after and right before the transition times imposed by the pulse. At these times the qubit state is described by $\mathbf{b}(t_l^+) = N_l \mathbf{b}(t_l^-)$, where the matrices N_l have the form³⁰⁾

$$N_l = \begin{pmatrix} \sqrt{1 - p_s} & \sqrt{p_s} \\ \sqrt{p_s} & \sqrt{1 - p_s} \end{pmatrix}, \quad (7)$$

where $\sqrt{1 - p_s} = \langle \psi_0^+ | \psi_C^- \rangle$ and $\sqrt{p_s} = \langle \psi_0^- | \psi_C^- \rangle$, the states $|\psi_{0,C}^\pm\rangle$ are the instantaneous eigenstates of the Eq. (1) without, 0, and with, C , the pulse application, more details can be found in Appendix A. The usual Landau-Zener transitions do not characterize the transition at the times t_1 and t_2 , where the pulse is applied. The pulse application discussed in this paper is an inherently diabatic process.

Concretely, the total evolution of the qubit state, starting at time 0, at the end of the annealing time, t_f , is described by,

$$|\psi(t_f)\rangle = U(t_f, t_2) N_2 U(t_2, t_1) N_1 U(t_1, 0) |\psi(0)\rangle \quad (8)$$

The transfer matrix model described in this paper is inspired by the adiabatic-impulse model,^{32–34)} describing the evolution of the quantum system considered, except at the times t_1 and t_2 where is described in the sudden approximation regime. The sudden approximation has been used to explain the Stuckelberg interference in superconducting qubits caused by periodic latching modulation.³⁰⁾ To our knowledge, it is the first time such physical explanation applied in the context of a QA protocol.

2.2 Tuning the success probability using the pulsed quantum annealing protocol for a single qubit

We start by investigating the PQA protocol for a single qubit, we present results from the full numerical and analytical methods introduced in the previous subsection. In Fig. 2 we present the SP, P_{SP} , for an annealing time $t_f = 10\hbar/\Delta$,

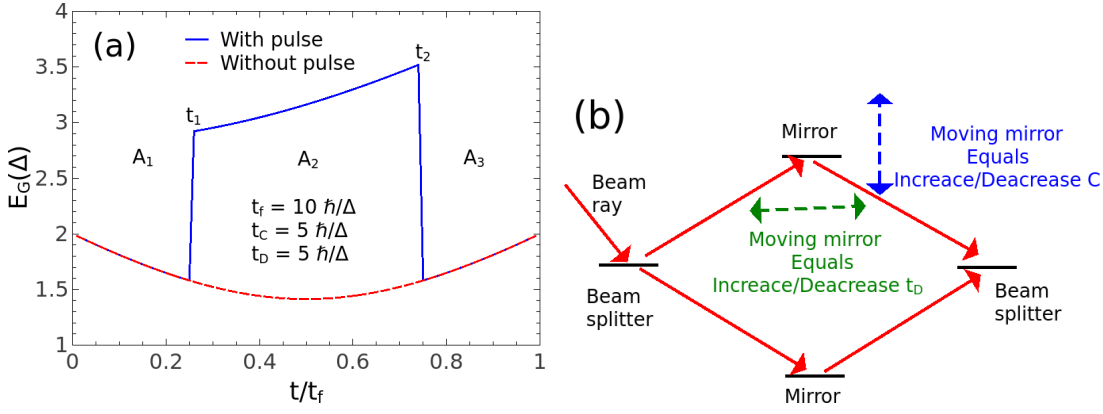


Fig. 1. (Color online) (a) The energy gap, $E_G(t)$, between the ground and the excited states for a single qubit by varying the time t during the annealing time $t_f = 10\hbar/\Delta$ and $\varepsilon = 1\Delta$. The blue continuous line gives the $E_G(t)$ in the presence of the pulse, with $t_c = 5\hbar/\Delta$, $t_D = 5\hbar/\Delta$ and $C = 1\Delta$, and the red dashed line for the $C = 0$ case of conventional QA. (b) The Mach-Zehnder interferometer and its analogy to the modulation of the success probability by a diabatic pulse application to a single qubit, of strength C and duration t_D .

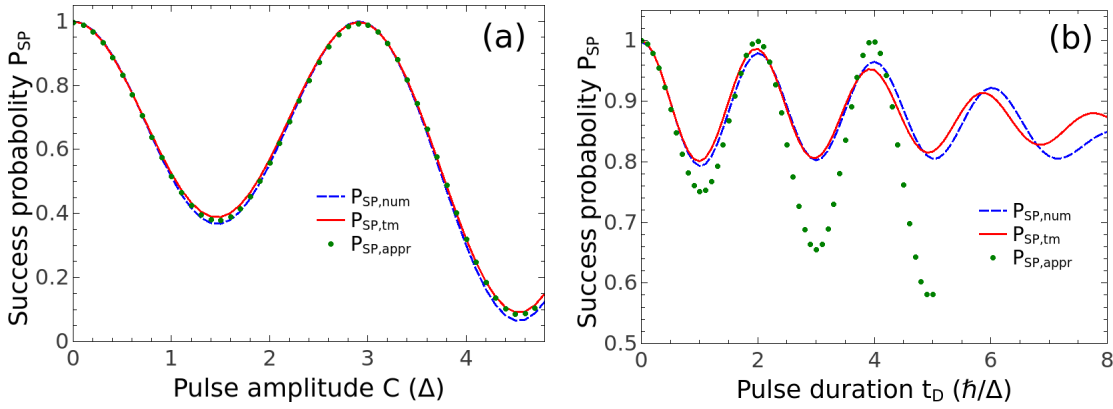


Fig. 2. (Color online) We present the success probability (SP), the probability of being occupied the ground state, of a qubit by varying the pulse parameters C and t_D , when the annealing time is $t_f = 10\hbar/\Delta$ and $\varepsilon = 1\Delta$, for which the adiabatic condition holds for $C = 0$. (a) The pulse amplitude C is varied for fixed pulse center $t_c = 1\hbar/\Delta$ and pulse duration $t_D = 1\hbar/\Delta$, (b) the pulse duration t_D is varied for fixed value of the pulse center $t_c = 5\hbar/\Delta$ and pulse amplitude $C = 1\Delta$. The blue dashed line gives the full numerical results, $P_{SP,num}$, the red continuous line the transfer matrix approach, $P_{SP,tm}$, and the green dots the approximate expression $P_{SP,appr}$.

for which the adiabatic condition for the conventional QA ($C = 0$) holds, and fixed $\varepsilon = 1\Delta$. In Fig. 2(a) we vary the pulse amplitude, C , for a fixed value of the pulse center, $t_c = 1\hbar/\Delta$, and of the pulse duration, $t_p = 1\hbar/\Delta$, while in Fig. 2(b) we vary the pulse duration, t_p , for fixed value of the pulse center, $t_c = 5\hbar/\Delta$, and of the pulse amplitude, $C = 1\Delta$. The blue dots give the SP for the case the Schrödinger equation is solved numerically, using the Hamiltonian of Eq. (1), and the red continuous line gives the results using the transfer matrix approach described earlier. We observe a good agreement between the two methods. The observed oscillations in the SP, P_{SP} , are due to destructive and constructive interference caused by the phase accumulation the qubit acquires during the pulse application. In Fig. 1(b) a direct analogy can be drawn with a Mach-Zehnder interferometer³⁵⁾ which is composed from two beam splitters. The first beam splitter divides the optical beam into two coherent beams that can follow different paths. The second beam splitter recombines and superimpose these beams, the different paths followed give interference fringes. To sum up, the pulse application due to interference effect, caused by the pulse application, can increase the SP for varying the pulse parameters. If we consider the

case that $\zeta_1(0, t_1) \approx \zeta_3(t_2, t_f)$ then the SP can be approximated by the expression $P_{SP,appr} = 1 - 4p_s(1 - p_s) \sin^2(\zeta_2(t_1, t_2))$. This approximate expression is plotted in Fig. 2 where we observe a reasonable agreement for the position of the maxima and minima of the SP.

In Fig. 2 we consider the case where the SP for the conventional QA is close to 1, implying that the adiabatic condition holds for $C = 0$. So now we focus on the case where we decrease the annealing time, $t_f = 5\hbar/\Delta$, and $\varepsilon = 0.5\Delta$, then the SP for the conventional QA is decreased to 0.89, due to the Landau-Zener transition. The minimum energy gap is $E_G^{min} = 0.22\Delta$ at $t_{min} = 4\hbar/\Delta$. Using Eq. (4) we find that the right hand side has the value $3.6\hbar/\Delta$ which is close to t_f , thus the adiabatic condition breaks. In Fig. 3 we present a contour plot of the SP, P_{SP} , for varying the values of the pulse amplitude, C , and the pulse duration, t_D , by keeping fixed the value of pulse center, $t_c = 2.5\hbar/\Delta$. We choose the pulse center value, t_c , so as to be at the center of the annealing time. The SP, P_{SP} , is increased, compared to its value for the conventional QA, up to values of 1. Furthermore, we observe that this increase is persisted for a wide range of the values of the pulse parameters implying the robustness of the proposed pro-

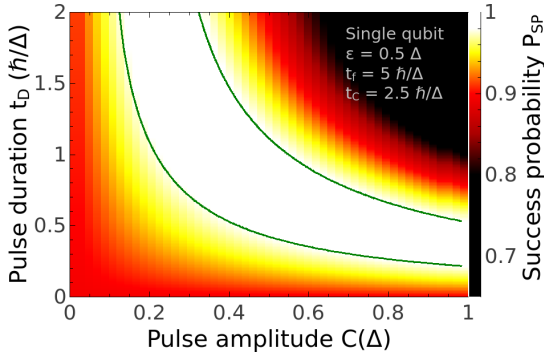


Fig. 3. (Color online) Contour plot of the success probability (SP), P_{SP} , of a single qubit for fixed annealing time, $t_f = 5\hbar/\Delta$, and pulse center, $t_C = 2.5\hbar/\Delta$, for varying the pulse amplitude, C , and the pulse duration, t_D . The energy difference between the ground and the excited states is $\varepsilon = 0.5\Delta$, at $C = 0$. The green line encloses the area where $P_{SP} > 0.98$. In the case of $C = 0$, the adiabatic condition does not hold.

tol. We also observe that for wider pulse durations, t_D , we need smaller values of the pulse amplitude in order to have an enhancement of the SP, compared to the $C = 0$ case. The position of the maxima of the SP are given by considering the maxima of the $P_{SP,appr}$, which are connected with the points at which $\zeta_2(t_1, t_2) = N\pi$, for $N = 0, 1, 2, \dots$. The full expression for the $\zeta_2(t_1, t_2)$, which can be analytically extracted from Eq. (6), has a complicate form and does not add anything to the discussion. In Fig. 3 we focus on the $N = 0$ case for later reference. The physical reason behind such result is the constructive interference effect due to the pulse application, which effect is used for increasing the SP for the multiqubit case as we see in the next section.

3. Increasing the success probability for multiqubit systems using pulsed quantum annealing

3.1 Multi-qubit model

We now expand the discussion for the single qubit case to the multiqubit case to investigate the pulsed quantum annealing (PQA) protocol. In the previous section we showed that changing the pulse parameters we can tune the SP for the case of a single qubit motivating the investigation of increasing the SP for the case of multiple qubits.

The Hamiltonian describing the PQA process for the multiqubit case is:

$$H = \frac{t}{t_f} H_t + C \Lambda_P(t) \sum_{i=1}^n \sigma_z^i + \left(1 - \frac{t}{t_f}\right) \Delta \sum_{i=1}^n \sigma_x^i, \quad (9)$$

the third term represents the quantum fluctuation part, with an amplitude Δ , the second term is the diagonally applied diabatic pulse, where the $\Lambda_P(t)$ scheduling is introduced in Eq. (1), with a strength C , and n is the number of qubits involved. The quantum fluctuation σ_x part gives a superposition state in the computational basis ($|0\rangle$ and $|1\rangle$), thus helps on exploring the energy landscape in order to find the ground state. The first term is the problem (spin-glass) Hamiltonian:

$$H_t = \sum_{i=1}^n \varepsilon_i \sigma_z^i + \sum_{i,j=1}^n J_{ij} \sigma_z^i \sigma_z^j, \quad (10)$$

where ε_i and J_{ij} are independent Gaussian random numbers with zero mean and variance $\langle J_{ij}^2 \rangle / \Delta^2 = \langle \varepsilon_i^2 \rangle / \Delta^2 = 1$.

Finding the ground state of H_t is connected with minimizing a cost function for an encoded optimization problem. However, in reality, long annealing times cause unwanted decoherence and dissipation effects, while short ones also induce nonadiabatic Landau-Zener transitions which reduce SP. Applying a diabatic pulse, like in the single qubit case, we can modulate the SP, of a multi-qubit system and, for specific pulse parameters, enhance it, for a fixed annealing time. We proceed by solving numerically the time-dependent Schrödinger equation Eq. (2) using the Hamiltonian Eq. (9) and its instantaneous eigenstates to calculate the SP, Eq. (3).

3.2 Five qubit example with low success probability

We start by studying the SP of a 5 qubit spin-glass instance, where for the conventional QA the SP is $P_{S0} = 0.47$, for an annealing time of $t_f = 10\hbar/\Delta$, for this instance the adiabatic condition does not hold. We name this instance as instance A (iA). In Fig. 4(a) we present the energy spectrum of iA for varying time t , we observe that the ground state, thick blue dashed line, is very close to the first excited state towards the end of the QA process, check the inset of Fig. 4(a), thus Landau-Zener transitions induce a reduction of the SP. In order to increase the SP we consider the effect of a single diabatic pulse application during the QA to the 5 qubit iA. In Fig. 4(b) the pulse parameters are $t_C = 5\hbar/\Delta$ and $t_D = 5\hbar/\Delta$, for the diabatic pulse center and duration respectively, while we vary the pulse strength C . We observe that due to interference effects, which are caused during the diabatic pulse application, the SP oscillates for varying the pulse amplitude C . This effect can be connected with the single qubit case, presented in Sec. 2, where varying the pulse amplitude induces constructive and destructive interference effects. For small pulse amplitudes, compared to the energy scale defined by the transition amplitude Δ , we observe that the SP increases compared to the conventional QA. Further increasing the value of the amplitude of the pulse amplitude, C , causes transitions to the higher excited states, thus reducing the SP at the end of the annealing time.

3.3 Multiple five qubit instances

From Fig. 4 it has become clear that if we want to increase the SP for the PQA, compared to the conventional QA, we need to find the appropriate parameter set of the applied pulse for each optimization problem. Let us define the SP when the pulse is applied as P_{SP} and without the pulse P_{S0} . In Fig. 5(a) we present a plot of P_{SP} to P_{S0} for 200 instances considering 5 qubits, for fixed annealing time $t_f = 10\hbar/\Delta$. For each instance we run a routine for optimizing the parameters of the pulse, which samples 2706 combinations for the pulse parameters for each instance, we define the maximum attained value of the SP as $P_{SP,max}$ and the averaged SP over all samplings per instance as $P_{SP,av}$. With blue dots we present the P_{SP}^{max} versus P_{S0} for each instance. The thick red line shows the $P_{SP} = P_{S0}$ diagonal line and is used as a guide for the reader, all instances that are above this line present an increase in the SP for the PQA compared to the conventional one. We observe that for all 200 instances exist a set of pulse parameters that can increase the attained value of the SP, even for the cases that the initial SP is $P_{S0} > 0.9$. The physical reason behind such a remarkable behavior is connected with the constructive interference during the diabatic pulse appli-

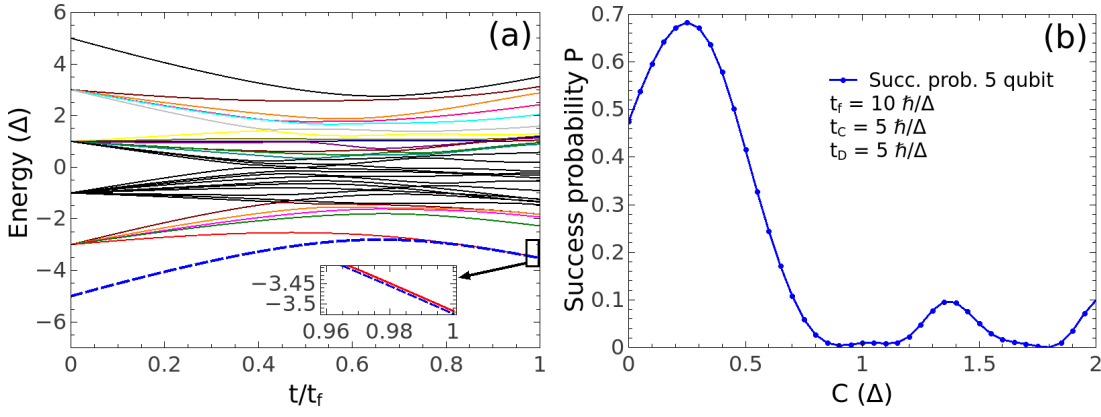


Fig. 4. (Color online) The success probability (SP) for the instance A of 5 qubits and annealing time of $t_f = 10\hbar/\Delta$. The SP for the conventional QA is $P_{S0} = 0.47$, for $t_f = 10\hbar/\Delta$. a) The energy spectrum of the 2^5 instantaneous eigenstates during the annealing without the pulse application. Inset: Energy spectrum of the two lowest energy levels close to the end of the annealing. b) The SP, P , for varying the diabatic pulse amplitude, C , with fixed pulse center $t_C = 5\hbar/\Delta$ and duration $t_D = 5\hbar/\Delta$.

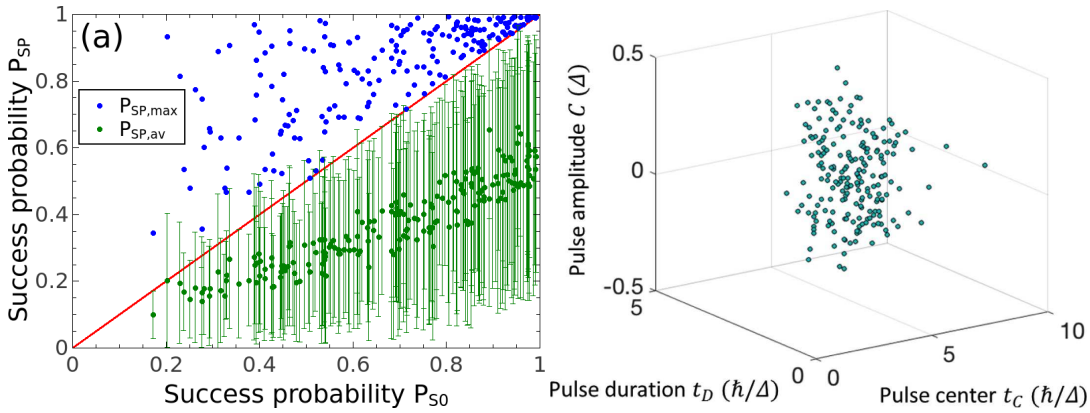


Fig. 5. (Color online) Plot of the success probability (SP) for 200 instances for the 5 qubit case, where the annealing time is $t_f = 10\hbar/\Delta$. a) SP with the diabatic pulse, P_{SP} , compared without, P_{S0} . Blue circles give the maximum attained SP, $P_{SP,max}$, while the green give the averaged SP for the total sampling, $P_{SP,av}$. The standard deviation is included as error bar in the figure. b) Averaged values of the pulse parameters, pulse center t_C , pulse duration t_D and pulse amplitude C for the parameter's value during the sampling that $P_{SP} > P_{S0}$.

cation, see Sec. 2 detailed explanation of the relevant physics, for the specific set of parameters for each instance.

In Fig. 5(a) the green dots present $P_{SP,av}$ versus P_{S0} for each instance, where we also show the standard deviation over the sampling for each instance as error bars. We observe that using the pulse application the average SP per instance $P_{SP,av}$ is reduced, compared to the conventional QA.

In Fig. 5(b) we present the average values of the pulse parameters for each instance that we have $P_{SP} > P_{S0}$, after the optimization routine, meaning that the pulsed QA gives higher SP than the conventional QA for fixed annealing time. We observe that the averaged pulse center has the value $t_C^{av} \sim t_f/2 = 5\hbar/\Delta$, which means that the optimum pulse center t_C is close to the middle of the annealing, from the single qubit case we can observe, Fig. ??(a), that the linear ramping of the conventional annealing leads to an avoided energy level crossing at around, and after, the $t/t_f \gtrsim 0.5$. Thus, applying a pulse where the avoided crossing exists is beneficial for creating a constructive interference.

Furthermore, we notice that the optimum amplitude parameter, $|C^{av}|$, is smaller than the energy scale defined by the tunneling amplitude Δ . Hence, the pulse amplitude modulation enhances the SP and can have a peak for small C value, com-

pared to Δ . Moreover, we observe that half of the generated instances are enhanced for the case we have positive pulse strength, C , while the other half of the instances for negative. Therefore, the enhancement of the SP is not due to the energy gap opening but due to the constructive interference during the pulse application. Based on the above remarks we can reduce the sampling parameter space considerably, considering mainly pulses of small amplitude C with a pulse center close to $t_f/2$, although we make a broader sampling for the pulse center. In Fig. 5 the sampling space is $O(10^3)$ after following the above remarks the sampling space can be reduced to $O(10^1)$.

In order to further understand the behavior of the PQA protocol we present in Fig. 6 a glassy instance for the 5 qubit system. After the optimization process, the parameters of the pulse enhancing the SP are: $t_C = 4\hbar/\Delta$, $t_D = 4\hbar/\Delta$ and $C = 0.3\Delta$. We name this instance as instance B (iB). In Fig. 6(a) we present the three lowest energy states of the iB, and in Fig. 6(b) we present the probability overlap of the ground, $i = 0$, and first excited, $i = 1$, instantaneous eigenstates to the system state evolution, $P_i(t) = |\langle\psi_i(t)|\psi(t)\rangle|^2$.

For the instance iB, we observe that there is a steep avoided crossing, Fig. 6(a), around $t/t_f = 0.4$, which cause a Landau-

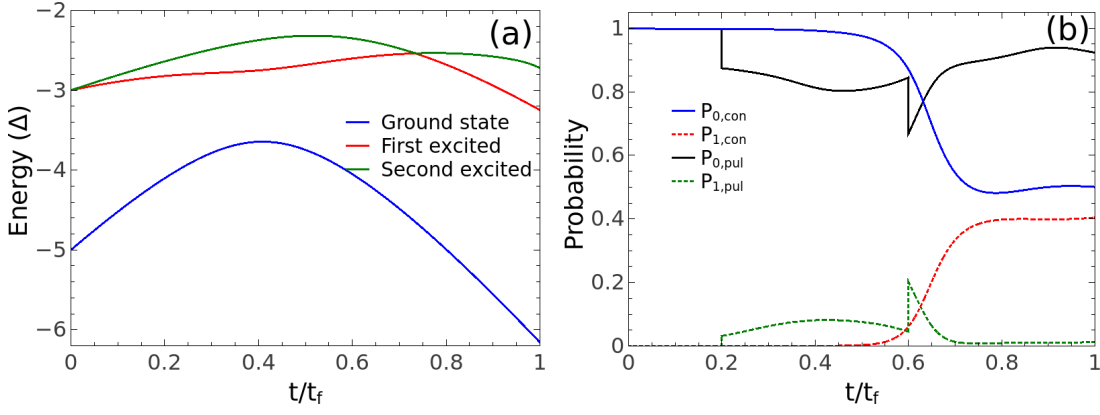


Fig. 6. (Color online) (a) The three lowest energy states and (b) the projection probability of the ground and excited instantaneous eigenstates to the system state $P_i(t) = |\langle \psi_i(t) | \psi(t) \rangle|^2$, for $i = 0, 1$ respectively. We consider the iB 5 qubit instance. $P_{i,con}(t)$ and $P_{i,pul}(t)$ are the state probability overlap for the conventional and pulsed QA, respectively. The annealing time is $t_f = 10\hbar/\Delta$.

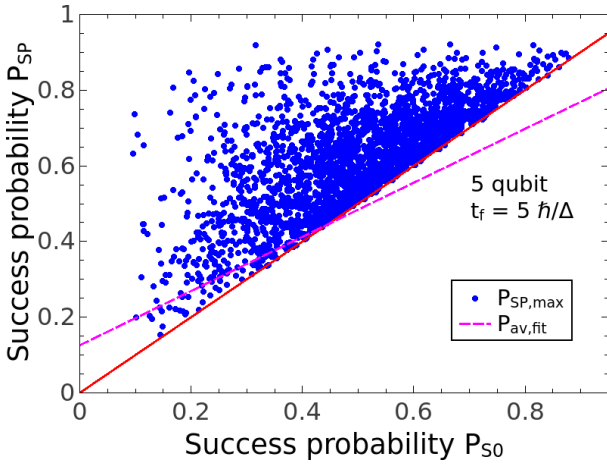


Fig. 7. (Color online) Plot of the success probability (SP) with the diabatic pulse, P_{SP} , compared without the pulse, P_{S0} , QA for 1000 instances for the 5 qubit case, the annealing time is $t_f = 5\hbar/\Delta$. The blue circles give the maximum attained SP, $P_{SP,max}$, to the P_{S0} . The magenta dashed line is a linear fitting of the $P_{SP,max}$ to the P_{S0} , $P_{SP,max} = A \cdot P_{S0} + B$, the linear fitting parameters are $A = 0.72$ and $B = 0.13$.

Zener transition that reduces the SP at the end of the annealing. The optimized pulse center, t_C , is at the avoided crossing. In Fig. 6(b) we observe that initially the system is at the ground state, until approaching the avoided crossing which causes a state mixing, between the ground and first excited states. This finally leads to a reduction of SP at the end of the annealing. In direct analogy with the single qubit case, presented in Sec. 2, the pulse application causes a constructive interference during the pulse application, leading to an increase in the SP at the end of the annealing, comparing to the conventional QA protocol for fixed annealing time.

The next step is to reduce the annealing time, t_f , in order to further reduce the SP for the conventional QA, thus allowing further space for enhancement for the PQA for showing clearly the importance of implementing the PQA protocol.

In Fig. 7 we present the SP for 1000 instances of 5 qubit systems, with the diabatic pulse application, P_{SP} , compared without the pulse, P_{S0} , for an annealing time of $t_f = 5\hbar/\Delta$; for this annealing time the adiabatic condition is violated for the conventional QA. The blue circles give the maximum attained

value of the SP, $P_{SP,max}$, where the sampling number for the pulse parameter optimization is just 90. We observe that the instances that $P_{SP,max} > P_{S0}$ is 100%, where on the same time for 80% of the instances we have $(P_{SP,max} - P_{S0})/P_{S0} > 5\%$. These results support that for fixed annealing times we can enhance the SP for specific set of pulse parameters for each instance.

In Fig. 7 we also present a linear fit, of the form $Ax + B$, of the averaged SP over the sampling of the pulse parameters, per instance $P_{SP,av}$ considering as $x = P_{S0}$. The linear fit parameters are $A = 0.72$ and $B = 0.13$. Moreover, in Fig. 7 we present the guide red line $P_{SP} = P_{S0}$ and we observe this line crosses the fitting of $P_{SP,av}$ vs P_{S0} . For the annealing time $t_f = 5\hbar/\Delta$ considered the cross is at $P_{S0}^c = 0.45$. For $P_{S0}^c > P_{S0}$ the averaged SP, $P_{SP,av}$, is increased for the case of pulsed over the conventional QA.

3.4 Scaling of success probability for the multi-qubit case

Up to now we focus on the case of 5 qubits to analyze and understand the influence of the diabatic pulse to the SP. It is desirable to investigate how the proposed diabatic PQA scales as the number of qubits n increases. We consider the cases of annealing time of $t_f = 5\hbar/\Delta$, with a sampling of the pulse parameters of 90 samples for each instance, where the the highest value for $P_{SP,max}$ per instance is recorded. In order to check this behavior we introduce the relative success probability per multiqubit system

$$R_{SP,max} = \frac{\bar{P}_{SP,max} - \bar{P}_{S0}}{\bar{P}_{S0}}, \quad (11)$$

where \bar{P} is the averaged SP over all instances and the sampling over the pulse parameters. $R_{SP,max}$ is a measure of how much the SP increases or decreases for the PQA compared to the conventional QA.

In Figs. 8a we present the value of $R_{SP,max}$, blue dots connected by blue lines, for increasing number of qubit n , for annealing times $t_f = 5\hbar/\Delta$. Instances of up to $n = 10$ qubits are considered. We observe that for increasing n the averaged $R_{SP,max}$ approaches a value of 30%. In Fig. 8b we present the averaged minimum energy between the ground and excited states by varying the qubit number n , where 10000 instances per qubit number have been averaged. We observe that the

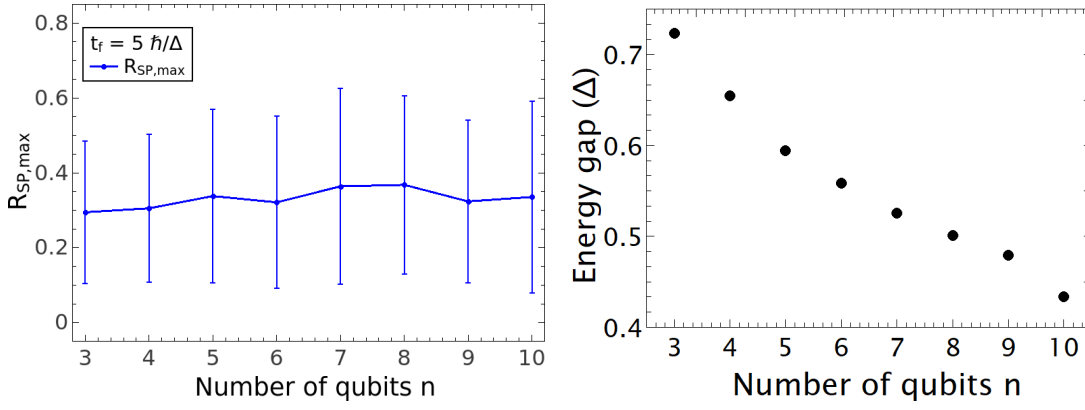


Fig. 8. (Color online) (a) Plot of the averaged relative success probability (SP), $R_{SP,max}$, for varying the number of qubits n . The standard deviation is presented as error bars, which is multiplied by 0.5. The annealing time is $t_f = 5\hbar/\Delta$. The numerical results are given as dots which are connected by lines in order to provide a guide to the eye. (b) Minimum of the energy gap between the ground and first excited state for varying the number of qubits n , each point is the average of 10000 random instances.

energy gap, between the ground and the first excited state, decreases as the number of qubits is increased, thus making it harder for the conventional quantum annealing to find the ground state, for the annealing time discussed in this section. The fact that the averaged SP $R_{SP,max}$ is positive shows that the PQA outperforms the conventional one. For an annealing time of $t_f = 5\hbar/\Delta$ the maximum relative SP, $R_{SP,max}$, shows a slight steady increase as the qubit number n increases. Of course the averaged relative SP, $R_{SP,max}$, suffers from high standard deviation, which is plotted as error bars in Fig. 8a, multiplied by 0.5.

The data presented in this paper are for up to $n = 10$ qubit systems, since we use a sampling to find the appropriate pulse parameters that provide an enhancement of the SP. We expect the scaling to sustain for increasing n , due to the fact that we consider a closed system at zero temperature. This approximation is justified for the short annealing times considered. In order to check the effectiveness of the PQA protocol for practical cases, e.g., D-Wave's quantum annealing machine, more detailed numerical study for large spin systems ($n > 10$) is needed. Such a systematic numerical study is an interesting future problem.

Finally it should be mentioned that the diabatic pulse introduced in the diagonal part of the Hamiltonian can be implemented in D-Wave superconducting quantum annealing machines based on a superconducting flux qubit.

4. Summary and Discussion

In this paper we start by investigating the success probability (SP) of a single qubit for the case of the conventional quantum annealing (QA) plus a diabatic pulse application. The diabatic pulse application can modulate the SP, by varying the pulse parameters, and enhance it for specific set of parameters. The constructive and destructive interference effect due to the acquired phase during the pulse application is the physical reason for such behavior of the system. Using the transfer matrix method, combined with the sudden approximation, we were able to present such an effect in a semi-analytical manner.

For the multiqubit cases, the pulse application can modulate the SP and for specific set of parameters we can increase the SP, compared to the conventional QA. When a number of

random (spin-glass) 5 qubit instances is considered, for each one of them we were able to increase the SP, for specific set of pulse parameters. Furthermore, reducing the annealing time, t_f , and based on the physical observations, that the avoided crossing emerges at times around and later from the middle of the annealing process, and consider pulse amplitudes smaller than the quantum fluctuations, we are able to reduce the sampling space.

As the number of qubits, n , is increased we have an enhancement of the SP. This enhancement seems to be constant although an improvement above 30% is persistent as the number of qubits is increased. This behavior is justified by the fact that increasing n the energy gap between the ground and excited states decreases, thus reducing the SP for the conventional QA, and giving space for larger enhancement for the PQA. This effect is studied by introducing the relative SP, R_{SP} , and investigate how this quantity behaves with increasing n . The averaged maximum attained SP, per sampling over all instances, per number of qubits shows better performance for the case of pulsed over the conventional QA after optimizing the pulse parameters.

The main message of our results is that breaking away from adiabaticity we are able to present an increase in the SP in shorter annealing times by applying a pulse. We have two sources for this increment. Reduction of the annealing time reduces the interaction of the system with the environment, thus reducing decoherence and dissipation effects. On the same time, reducing the annealing time significantly we can run the appropriate number of samplings, while increasing the SP, within a reasonable time frame.

Recently, D-Wave Systems Inc. announced the implementation of the reverse QA protocol,³⁸⁾ where the initial state is not the usual ground state of the quantum fluctuations, but a specific state which might be closer to the ground state of the problem Hamiltonian. In Ref.³⁹⁾ it is proposed a hybrid computing method where initially a classical algorithm, like simulated annealing, can be used to find a solution close to the real ground state of a complicated problem. Then, this state can be used as the initial state for applying the reverse QA protocol for a local search in the phase space. The PQA protocol can also be used in a similar manner, to provide if not the real ground state, a state very close to it. This is a differ-

ent research path to follow in the future for a PQA machine application.

One year after submitting our manuscript in arXiv:1806.08517 (submission date 22 Jun. 2018) we became aware of ref.⁴⁰⁾ (submission date 18 March 2019) where PQA for only the single qubit case was investigated using the interferometer-interpretation we gave in Fig. 1(b).

The authors would like to thank K. Imafuku, M. Maezawa, Y. Seki, and S. Tanaka for useful discussions. This work is based on results obtained from a project commissioned by the New Energy and Industrial Technology Development Organization (NEDO), Japan.

Appendix: Sudden approximation

Following the refs.^{30,31)} let's consider the case where we have the diabatic pulse application at the time t_1 , for times $t < t_1$ the Hamiltonian has the form

$$H_0(t) = \begin{pmatrix} t/t_f \varepsilon & (1 - t/t_f) \Delta \\ (1 - t/t_f) \Delta & -t/t_f \varepsilon \end{pmatrix} \quad (\text{A.1})$$

$$= E_G^0(t) \begin{pmatrix} \cos(\theta_0(t)) & \sin(\theta_0(t)) \\ \sin(\theta_0(t)) & -\cos(\theta_0(t)) \end{pmatrix},$$

where we define $\cos(\theta_0(t)) = (t/t_f) \varepsilon / E_G^0(t)$ and $\sin(\theta_0(t)) = (1 - t/t_f) \Delta / E_G^0(t)$, $E_G^0(t) = \sqrt{(t/t_f)^2 \varepsilon^2 + (1 - t/t_f)^2 \Delta^2}$ is the energy gap between the ground and the excited states. The relevant eigenstates are

$$|\psi_0^-(t)\rangle = \begin{pmatrix} -\sin(\theta_0(t)/2) \\ \cos(\theta_0(t)/2) \end{pmatrix}, \quad |\psi_0^+(t)\rangle = \begin{pmatrix} \cos(\theta_0(t)/2) \\ \sin(\theta_0(t)/2) \end{pmatrix}, \quad (\text{A.2})$$

where $|\psi_0^-(t)\rangle$ is the ground and $|\psi_0^+(t)\rangle$ the excited states. Similarly for $t > t_1$ we have the Hamiltonian

$$H_C(t) = \begin{pmatrix} t/t_f \varepsilon + C & (1 - t/t_f) \Delta \\ (1 - t/t_f) \Delta & -t/t_f \varepsilon - C \end{pmatrix} \quad (\text{A.3})$$

$$= E_G^C(t) \begin{pmatrix} \cos(\theta_C(t)) & \sin(\theta_C(t)) \\ \sin(\theta_C(t)) & -\cos(\theta_C(t)) \end{pmatrix},$$

where we defined $\cos(\theta_C(t)) = (t/t_f \varepsilon + C) / E_G^C(t)$ and $\sin(\theta_C(t)) = (1 - t/t_f) \Delta / E_G^C(t)$, $E_G^C(t) = \sqrt{(t/t_f \varepsilon + C)^2 + (1 - t/t_f)^2 \Delta^2}$ is the energy gap between the ground and the excited states in the presence of the pulse of amplitude C . The relevant eigenvectors are

$$|\psi_C^-(t)\rangle = \begin{pmatrix} -\sin(\theta_C(t)/2) \\ \cos(\theta_C(t)/2) \end{pmatrix}, \quad |\psi_C^+(t)\rangle = \begin{pmatrix} \cos(\theta_C(t)/2) \\ \sin(\theta_C(t)/2) \end{pmatrix}, \quad (\text{A.4})$$

where $|\psi_C^-(t)\rangle$ is the ground and $|\psi_C^+(t)\rangle$ the excited states.

At the time $t = t_1$ due to the sudden transition of the Hamiltonian from the form $H_0(t)$ to $H_C(t)$ the system stays in the same state, then the matrix N_1 can be used to describe the transition from the basis $|\psi_0^\pm(t = t_1)\rangle$ to the basis $|\psi_C^\pm(t = t_1)\rangle$, thus the relevant state mixing between the ground and the excited states. The elements of the matrix N_1 are $\sqrt{p_s} = \sin(\theta_C(t_1) - \theta_0(t_1))$ and $\sqrt{1 - p_s} = \cos(\theta_C(t_1) - \theta_0(t_1))$ and

the system state, $\mathbf{b}(t) = \begin{pmatrix} b_0(t) \\ b_1(t) \end{pmatrix}$, at t_1^+ is given by

$$\begin{pmatrix} b_0(t_1^+) \\ b_1(t_1^+) \end{pmatrix} = \begin{pmatrix} \sqrt{1 - p_s} & \sqrt{p_s} \\ \sqrt{p_s} & \sqrt{1 - p_s} \end{pmatrix} \begin{pmatrix} b_0(t_1^-) \\ b_1(t_1^-) \end{pmatrix}. \quad (\text{A.5})$$

Most of the readers would anticipate the physical evolution of the system under the QA protocol to be determined by the Landau-Zener transitions. Then, at the diabatic pulse application times the faulty impression is that we would had a transition to the excited state with probability 1. This is wrong as we can see from the full numerical data and the explanation given from the transfer matrix approach, using the sudden approximation. The pulse application discussed in this paper is a diabatic process thus the effect of the Landau-Zener physics is irrelevant at t_1 and t_2 .

- 1) T. Kadowaki and H. Nishimori, Phys. Rev. E **58**, 5355 (1998).
- 2) E. Farhi, J. Goldstone, S. Gutmann, J. Lapan, A. Lundgren, and D. Preda, Science **292**, 472 (2001).
- 3) S. Kirkpatrick, C. D. Gelatt, and M.P. Vecchi, Science **220**, 671 (1983).
- 4) A. Das and B.K. Chakrabarti, Rev. Mod. Phys. **80**, 1061 (2008).
- 5) R. Harris, M.W. Johnson, T. Lanting, A.J. Berkley, J. Johansson, P. Bunyk, E. Tolkacheva, E. Ladizinsky, N. Ladizinsky, T. Oh, F. Cioata, I. Perminov, P. Spear, C. Enderud, C. Rich, S. Uchaikin, M. C. Thom, E. M. Chapple, J. Wang, B. Wilson, M. H. S. Amin, N. Dickson, K. Karimi, B. Macready, C.J.S. Truncik and G. Rose, Phys. Rev. B **82**, 024511 (2010).
- 6) M. W. Johnson, M. H. S. Amin, S. Gildert, T. Lanting, F. Hamze, N. Dickson, R. Harris, A. J. Berkley, J. Johansson, P. Bunyk, E. M. Chapple, C. Enderud, J. P. Hilton, K. Karimi, E. Ladizinsky, N. Ladizinsky, T. Oh, I. Perminov, C. Rich, M. C. Thom, E. Tolkacheva, C. J. S. Truncik, S. Uchaikin, J. Wang, B. Wilson, and G. Rose, Nature **473**, 194 (2011).
- 7) N. G. Dickson, M. W. Johnson, M. H. Amin, R. Harris, F. Altomare, A. J. Berkley, P. Bunyk, J. Cai, E.M. Chapple, P. Chavez, F. Cioata, T. Cirip, P. DeBuen, M. Drew-Brook, C. Enderud, S. Gildert, F. Hamze, J. P. Hilton, E. Hoskinson, K. Karimi, E. Ladizinsky, N. Ladizinsky, T. Lanting, T. Mahon, R. Neufeld, T. Oh, I. Perminov, C. Petroff, A. Przybysz, C. Rich, P. Spear, A. Tcaciuc, M.C. Thom, E. Tolkacheva, S. Uchaikin, J. Wang, A. B. Wilson, Z. Merali, and G. Rose, Nat. Commun. **4**, 1903 (2013).
- 8) J. Raymond, S. Yarkoni, and E. Andriyash, Frontiers in ICT **3**, 23 (2016).
- 9) F. Neukart, G. Compostella, C. Seidel, D. von Dollen, S. Yarkoni, and B. Parney, Frontiers in ICT **4**, 29 (2017).
- 10) M. Henderson, J. Novak, and T. Cook, J. Phys. Soc. Jpn. **88**, 061009 (2019).
- 11) K. Tanahashi, S. Takayanagi, T. Motohashi, and S. Tanaka, J. Phys. Soc. Jpn. **88**, 061010 (2019).
- 12) A. Mott, J. Job, J.-R. Vlimant, D. Lidar, and M. Spiropulu, Nature **550**, 375 (2017).
- 13) R. Barends, A. Shabani, L. Lamata, J. Kelly, A. Mezzacapo, U. Las Heras, R. Babbush, A. G. Fowler, B. Campbell, Yu Chen, Z. Chen, B. Chiaro, A. Dunsworth, E. Jeffrey, E. Lucero, A. Megrant, J. Mutus, M. Neeley, C. Neill, P. J. J. O'Malley, C. Quintana, P. Roushan, D. Sank, A. Vainsencher, J. Wenner, T.C. White, E. Solano, H. Neven, and J. M. Martinis, Nature **534**, 222 (2016).
- 14) M. Maezawa, K. Imafuku, M. Hidaka, H. Koike, S. Kawabata, IEEE Conf. Proc. 16th Int. Superconductive Electronics Conf. (2017), arXiv:1712.05561 (2017).
- 15) S. J. Weber, G. O. Samach, D. Hover, S. Gustavsson, D. K. Kim, A. Melville, D. Rosenberg, A. P. Sears, F. Yan, J. L. Yoder, W. D. Oliver, and A. J. Kerman, Phys. Rev. Applied **8**, 014004 (2017).
- 16) S. Novikov, R. Hinkey, S. Disseler, J. I. Basham, T. Albash, A. Risinger, D. Ferguson, D. A. Lidar, K. M. Zick, arXiv:1809.04485 (2018).
- 17) H. Mukai, A. Tomonaga, and J.-S. Tsai, J. Phys. Soc. Jpn. **88**, 061011 (2019).
- 18) M. Maezawa, G. Fujii, M. Hidaka, K. Imafuku, K. Kikuchi, H. Koike, K. Makise, S. Nagasawa, H. Nakagawa, M. Ukiye, S. Kawabata, J. Phys. Soc. Jpn. **88**, 061012 (2019).
- 19) T. Tanamoto, Y. Nishi, and J. Deguchi, J. Phys. Soc. Jpn. **88**, 061013 (2019).

- 20) H. Goto, J. Phys. Soc. Jpn. **88**, 061015 (2019).
- 21) T. Albash and D.A. Lidar, Rev. Mod. Phys. **90**, 015002 (2018).
- 22) T. Albash and D.A. Lidar, Phys. Rev. A **91**, 062320 (2015).
- 23) D.S. Steiger, T.F. Rønnow, and M. Troyer, Phys. Rev. Lett. **115**, 230501 (2015).
- 24) E. Crosson, E. Farhi, C. Y.-Y. Lin, H.-H. Lin, and P. Shor, arXiv:1401.7320 (2014).
- 25) S. N. Shevchenko, S. Ashhab, and F. Nori, Phys. Rep. **492**, 1 (2010).
- 26) C. Zener, Proceedings of the Royal Society A: Mathematical, Physical and Engineering Sciences **137**, 696 (1932).
- 27) N. V. Vitanov and B. M. Garraway, Phys. Rev. A **53**, 4288 (1996).
- 28) S. Ashhab, J. R. Johansson, A. M. Zagoskin, and F. Nori, Phys. Rev. A **75**, 063414 (2007).
- 29) J. Zhou, P. Huang, Q. Zhang, Z. Wang, T. Tan, X. Xu, F. Shi, X. Rong, S. Ashhab, and J. Du, Phys. Rev. Lett. **112**, 010503 (2014).
- 30) M. P. Silveri, K. S. Kumar, J. Tuorila, J. Li, A. Vepsäläinen, E. V. Thuneberg, and G. S. Paraoanu, New J. Phys. **17**, 043058 (2015).
- 31) A. Messiah, Quantum Mechanics, (Dover Books, 2014).
- 32) B. M. Garraway and N. V. Vitanov, Phys. Rev. A **55**, 4418 (1997).
- 33) B. Damski, Phys. Rev. Lett. **95**, 035701 (2005).
- 34) B. Damski and W. H. Zurek, Phys. Rev. A **73**, 063405 (2006).
- 35) W. D. Oliver, Science **310**, 1653 (2005).
- 36) M. Sillanpää, T. Lehtinen, A. Paila, Y. Makhlin, and P. Hakonen, Phys. Rev. Lett. **96**, 187002 (2006).
- 37) A. Izmailkov, S. H. W. van der Ploeg, S. N. Shevchenko, M. Grajcar, E. Il'ichev, U. Hübner, A. N. Omelyanchouk, and H. -G. Meyer, Phys. Rev. Lett. **101**, 017003 (2008).
- 38) D-Wave Whitepaper Series, 14-1018A-A (2017).
- 39) N. Chancellor, New J. Phys. **19**, 023024 (2017).
- 40) H. Munoz-Bauza, H. Chen, and Daniel Lidar, npj Quant. Information **5**, 2 (2019).